Journal of the Korean Physical Society, Vol. 66, No. 7, April 2015, pp. 1093∼1096

Effects of Zn^{2+} and Mn^{4+} Co-doping in $BiFeO_3$ Thin Films

Dalhyun Do*

Department of Advanced Materials Engineering, Keimyung University, Daegu 704-701, Korea

(Received 28 April 2014, in final form 24 December 2014)

$Bi(Fe_{0.99-x}Zn_{0.01}Mn_x)O_3$ (x = 0.01, 0.03, 0.05) thin films were deposited on Pt(111)/Ti/SiO_2/Si(100) substrates by using a pulsed laser deposition method. The effects of Mn^{4+} content in the $BiFeO_3$ thin films on their leakage current and their ferroelectric properties were mainly investigated. $Bi(Fe_{0.96}Zn_{0.01}Mn_{0.03})O_3$ thin film exhibited the best ferroelectric properties among them. The leakage current density of the film capacitor was 2.0×10^{-5} A/cm^2 at 200 kV/cm. The remnant polarization ($2P_r$) and the coercive electric field ($2E_c$) of the film capacitor were 83 μC/cm^2 and 577 kV/cm at an applied electric field of 695 kV/cm, respectively. This can be explained based on the Fe^{2+} concentration associated with oxygen vacancies and the grain size caused by doping of Zn^{2+} and Mn^{4+} in $BiFeO_3$ thin films.

PACS numbers: 77.22.Ej, 77.55.+f, 77.80.Dj, 77.80.-e
Keywords: Ferroelectric, $BiFeO_3$, Doping
DOI: 10.3938/jkps.66.1093

I. INTRODUCTION

Multiferroic materials have simultaneous ferroelectricity and ferromagnetism, which can be potentially utilized for magnetoelectronic devices. $BiFeO_3$ (BFO) has been extensively studied due to its room-temperature multiferroic properties [1, 2]. However, BFO suffers from a high leakage current because of the existence of Fe^{2+} ions and oxygen vacancies [3]. Reports indicate that the formation of Fe^{2+} and the creation of oxygen vacancies can be controlled by doping or substitution at the Fe sites in BFO. Doping of 4+ ions is expected to decrease the creation of oxygen vacancies, and the doping of 2+ ions is expected to prevent the formation of Fe^{2+} ions [4]. Compared to BFO thin films, reduced leakage current density was observed in Zn^{2+}-doped BFO thin films and Ti^{4+}-doped BFO thin films [5–7]. In the case of Mn-doped BFO thin films, the valence state of Mn is important because Mn is a multivalent element. The BFO thin film with Mn^{4+} doping exhibits a much lower leakage current density than the Mn^{2+}-doped BFO thin film does, which is related to the concentration of oxygen vacancies [8,9]. On the other hand, oxygen vacancies can form defect complexes with other negatively-charged defects such as Zn^{2+} in the Fe^{3+} sites. In Zn^{2+}-doped BFO thin films, the leakage current has been reported to be reduced with increasing formation of defect complexes between oxygen vacancies and Zn^{2+} in Fe^{3+} sites [10]. Thus, an effective way to reduce the leakage current in BFO may be to eliminate oxygen vacancies by the introduction of 4+ ions at the Fe sites and by the formation of defect complexes.

In this study, we prepared $Bi(Fe_{0.99-x}Zn^{2+}_{0.01}Mn^{4+}_x)O_3$ (x = 0.01, 0.03, 0.05) thin films by using a pulsed laser deposition method. The dependences of the leakage current and the ferroelectric properties on the Mn^{4+} content were investigated, and the $Bi(Fe_{0.96}Zn_{0.01}Mn_{0.03})O_3$ thin film was found to show the lowest leakage current density and the largest remnant polarization, which is related to the Fe^{2+} concentration associated with oxygen vacancies and grain size. This provides some important information about control of the leakage current in doped-BFO thin films.

II. EXPERIMENTS AND DISCUSSION

$Bi(Fe_{0.99-x}Zn_{0.01}Mn_x)O_3$ (x = 0.01, 0.03, 0.05) thin films were deposited on Pt(111)/Ti/SiO_2/Si(100) substrates by using a pulsed laser deposition (PLD) method. PLD targets with 5% Bi excess were prepared by using a traditional solid-state reaction with Bi_2O_3 (99.999%, Sigma-Aldrich), Fe_2O_3 (99.999%, Sigma-Aldrich), MnO_2 (99.99%, Sigma-Aldrich), and ZnO (99.9%, Sigma-Aldrich) powders. A KrF excimer laser with a wavelength of 248 nm and a repetition rate of 5 Hz was used to ablate the targets. The laser's energy density was about 1.7 J/cm^2 per pulse. During the deposition of the films, the substrate temperature was kept at 520 °C under an oxygen partial pressure of 30 mTorr. After deposition, the films were cooled to room temperature under an oxygen partial pressure of 760 Torr.

*E-mail: ddo@kmu.ac.kr; Fax: +82-53-580-5165

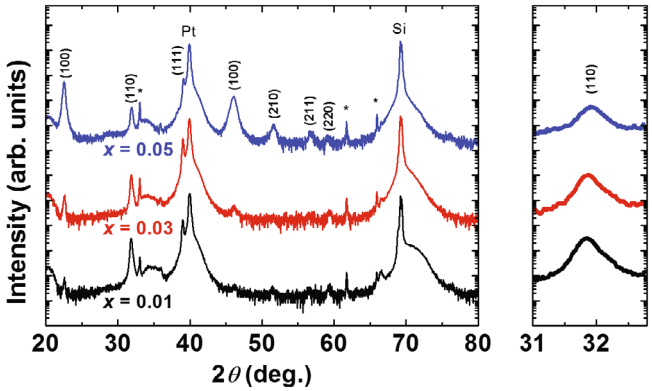

Fig. 1. (Color online) XRD patterns of $Bi(Fe_{0.99-x}Zn_{0.01}Mn_x)O_3$ (x = 0.01, 0.03, 0.05) thin films. The "*" indicates substrate peaks.

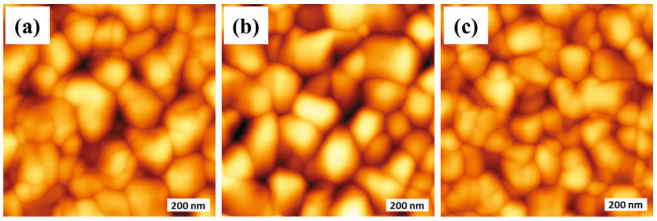

Fig. 2. (Color online) AFM images of the surface morphology of (a) x = 0.01, (b) x = 0.03, and (c) x = 0.05 $Bi(Fe_{0.99-x}Zn_{0.01}Mn_x)O_3$ thin films. The size of each image is 1 μm × 1 μm.

The crystal structure and the microstructure of the films were investigated by using X-ray diffraction (XRD) equipment (Rigaku, MiniFlex II) and atomic force microscopy (AFM, Park Systems, XE7), respectively. The oxidation states of the Fe ions were measured by using X-ray photoelectric spectroscopy (XPS, VG Scientifics, ESCALAB 250, Korea Basic Science Institute, Busan Center). The ferroelectric hysteresis loops and the leakage current density were measured by using a modified Sawyer-Tower circuit and a semiconductor parameter analyzer (HP 4145b), respectively. For electrical measurements, Pt top electrodes were deposited on the tops of the films by using ion sputtering through a shadow mask.

Figure 1 shows XRD patterns of $Bi(Fe_{0.99-x}Zn_{0.01}Mn_x)O_3$ (x = 0.01, 0.03, 0.05) thin films deposited on $Pt(111)/Ti/SiO_2/Si(100)$ substrates. The diffraction peaks were indexed based on the pseudocubic structure of BFO. Compared to the crystal structure of BFO thin films [11], no significant changes in the crystal structure were observed because the ionic radii of the Zn^{2+} and the Mn^{4+} ions are close to that of the Fe^{3+} ions [12]. No impurity peaks were observed in the XRD patterns, indicating that the Zn and the Mn ions were well-substituted into BFO. The $Bi(Fe_{0.94}Zn_{0.01}Mn_{0.05})O_3$ (110) reflection was shifted to higher 2θ angle, indicating that the lattice constant of $Bi(Fe_{0.94}Zn_{0.01}Mn_{0.05})O_3$ had become smaller than those of $Bi(Fe_{0.98}Zn_{0.01}Mn_{0.01})O_3$ and $Bi(Fe_{0.96}Zn_{0.01}Mn_{0.03})O_3$ because the $Bi(Fe_{0.94}Zn_{0.01}Mn_{0.05})O_3$ thin film has the largest number of Fe^{2+} ions, whose radius is smaller than that of Fe^{3+} ions, as shown in Fig. 3.

AFM images of the surface morphologies of the films are shown in Fig. 2. The shapes of the grains were irregular. Small grains were merged to form larger grains for the $Bi(Fe_{0.98}Zn_{0.01}Mn_{0.01})O_3$ and the $Bi(Fe_{0.94}Zn_{0.01}Mn_{0.05})O_3$ thin films. However, this was not observed in the $Bi(Fe_{0.96}Zn_{0.01}Mn_{0.03})O_3$ thin film. The average grain size of the $Bi(Fe_{0.96}Zn_{0.01}Mn_{0.03})O_3$ thin film was approximately 170 nm in diameter, which is larger than those of the $Bi(Fe_{0.98}Zn_{0.01}Mn_{0.01})O_3$ and the $Bi(Fe_{0.94}Zn_{0.01}Mn_{0.05})O_3$ thin films, indicating that the lowest leakage current may be expected in the $Bi(Fe_{0.96}Zn_{0.01}Mn_{0.03})O_3$ thin film. The thicknesses of $Bi(Fe_{0.99-x}Zn_{0.01}Mn_x)O_3$ (x = 0.01, 0.03, 0.05) thin films were 718, 614, and 679 nm, respectively.

Figure 3 shows XPS data for the oxidation states of the films. The binding energy of the $2P_{3/2}$ state is 709.5 eV for Fe^{2+} and 711.0 eV for Fe^{3+} [4]. The volume fractions of Fe^{2+} and Fe^{3+} were estimated by using the XPSPEAK 4.1 software, as shown in Figs. 3(a)−(c). The fractions of Fe^{2+} were 28%, 25%, and 31% for the $Bi(Fe_{0.99-x}Zn_{0.01}Mn_x)O_3$ (x = 0.01, 0.03, 0.05) thin films, respectively, as shown in Fig. 3(d). With increasing Mn^{4+} content, the Fe^{2+} concentration is reported to increase, and the oxygen vacancy concentration to decrease [4]. However, in the case of the $Bi(Fe_{0.96}Zn_{0.01}Mn_{0.03})O_3$ thin film, the concentration of Fe^{2+} is lower than that of the $Bi(Fe_{0.98}Zn_{0.01}Mn_{0.01})O_3$ thin film. The full width at half maximum of the Fe^{3+} peak of the $Bi(Fe_{0.96}Zn_{0.01}Mn_{0.03})O_3$ thin film (Fig. 3(b)) is wider than that of the other films. Fe^{4+} ions may have been creating, thus resulting in a reduced Fe^{2+} concentration.

Figure 4 shows the leakage current density as a function of the applied electric field measured at room temperature. The leakage current density of the $Bi(Fe_{0.99-x}Zn_{0.01}Mn_x)O_3$ (x = 0.01, 0.03, 0.05) thin-film capacitors were much lower than that of $BiFeO_3$ thin-film capacitor [11]. The values of the leakage current densities of the $Bi(Fe_{0.99-x}Zn_{0.01}Mn_x)O_3$ (x = 0.01, 0.03, 0.05) thin-film capacitors were 1.6 × 10^{-4}, 2.0 × 10^{-5}, and 3.9 × 10^{-4} A/cm^2 at 200 kV/cm, respectively. The $Bi(Fe_{0.96}Zn_{0.01}Mn_{0.03})O_3$ thin film exhibited the lowest leakage current density among them. The reduced leakage current observed in the $Bi(Fe_{0.96}Zn_{0.01}Mn_{0.03})O_3$ thin film could have originated from the small Fe^{2+} concentration. Thus, fewer oxygen vacancies existed in the $Bi(Fe_{0.96}Zn_{0.01}Mn_{0.03})O_3$ thin film. Another origin is the large grain size observed in the $Bi(Fe_{0.96}Zn_{0.01}Mn_{0.03})O_3$ thin film, as shown in Fig. 2(b). In the low-electric-field region, a lower leakage current was observed in the $Bi(Fe_{0.98}Zn_{0.01}Mn_{0.01})O_3$ thin film than in the

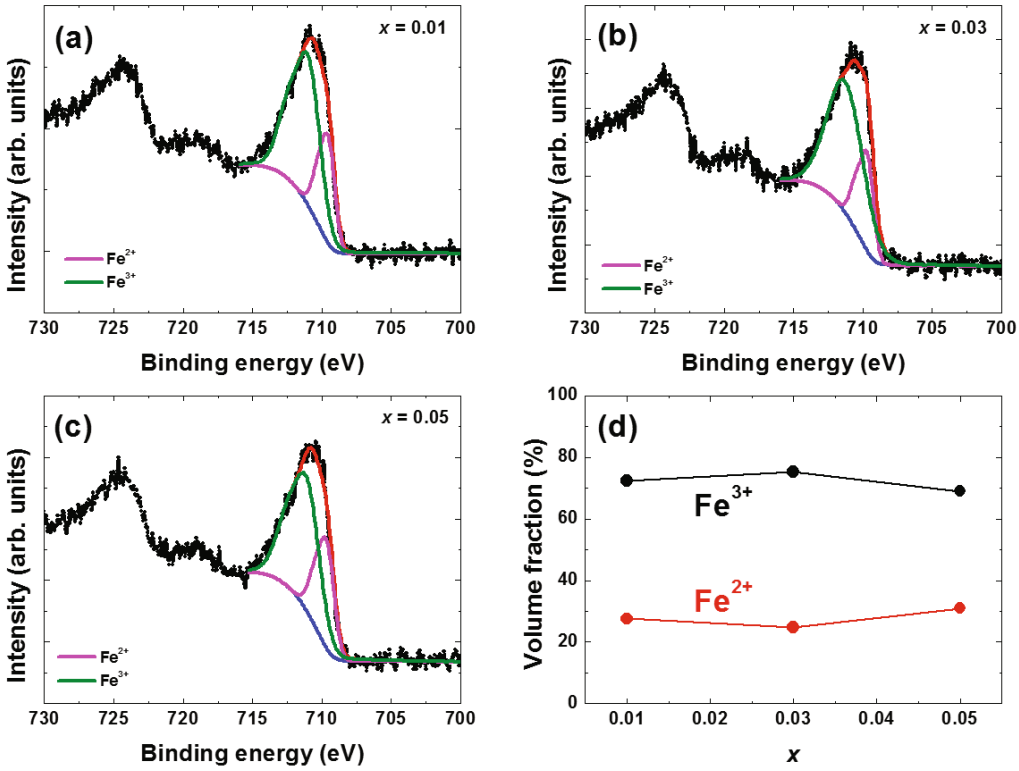

Fig. 3. (Color online) XPS results of (a) $x = 0.01$, (b) $x = 0.03$, and (c) $x = 0.05$ $Bi(Fe_{0.99-x}Zn_{0.01}Mn_x)O_3$ thin films, and (d) volume fractions of Fe^{3+} and Fe^{2+} of $Bi(Fe_{0.99-x}Zn_{0.01}Mn_x)O_3$ ($x = 0.01$, 0.03, 0.05) thin films.

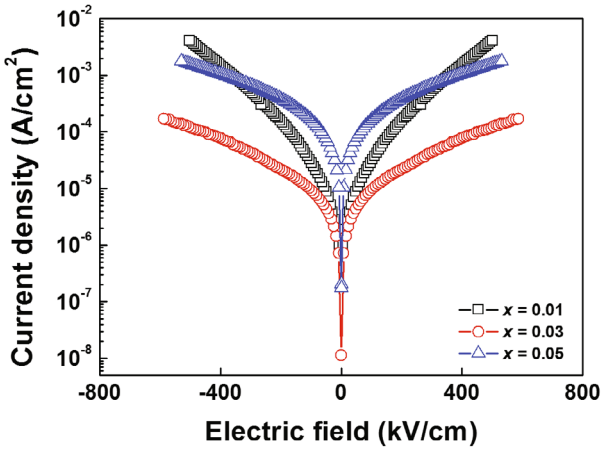

Fig. 4. (Color online) Leakage current density as a function of applied electric field for $Bi(Fe_{0.99-x}Zn_{0.01}Mn_x)O_3$ ($x = 0.01$, 0.03, 0.05) thin-film capacitors measured at room temperature.

$Bi(Fe_{0.94}Zn_{0.01}Mn_{0.05})O_3$ thin film whereas the leakage current of the $Bi(Fe_{0.98}Zn_{0.01}Mn_{0.01})O_3$ thin film was higher in the high-electric-field region. This could be explained by the observation that the defect complexes formed between the oxygen vacancies and Zn^{2+} ions at the Fe^{3+} sites in the $Bi(Fe_{0.98}Zn_{0.01}Mn_{0.01})O_3$ thin film can be more easily release, compared with the $Bi(Fe_{0.94}Zn_{0.01}Mn_{0.05})O_3$ thin film, with increasing electric field.

Figures 5(a)−(c) shows the frequency-dependent ferroelectric hysteresis loops of $Bi(Fe_{0.99-x}Zn_{0.01}Mn_x)O_3$ ($x = 0.01$, 0.03, 0.05) thin-film capacitors. The loops were measured by using a triangular voltage pulse with a frequency of 1, 10, or 100 kHz. The loops at 1 kHz were leaky while the loops at 10 and 100 kHz were saturated. Figure 5(d) shows the ferroelectric hysteresis loops of the $Bi(Fe_{0.99-x}Zn_{0.01}Mn_x)O_3$ ($x = 0.01$, 0.03, 0.05) thin-film capacitors measured under a 10 kHz triangular voltage pulse. All films showed well-saturated loops. The values of the remnant polarization ($2P_r$) of the $Bi(Fe_{0.99-x}Zn_{0.01}Mn_x)O_3$ ($x = 0.01$, 0.03, 0.05) thin-film capacitors were 59, 83, and 49 $\mu C/cm^2$, respectively. The values of the coercive electric field ($2E_c$) were 523, 577, and 558 kV/cm, respectively. Among the films investigated in this study, the $Bi(Fe_{0.96}Zn_{0.01}Mn_{0.03})O_3$ thin film exhibited the best ferroelectric properties due to its low leakage current.

III. CONCLUSION

In summary, $Bi(Fe_{0.99-x}Zn_{0.01}Mn_x)O_3$ ($x = 0.01$, 0.03, 0.05) thin films were deposited on Pt(111)/$Ti/SiO_2/Si(100)$ substrates by using a pulsed laser de-

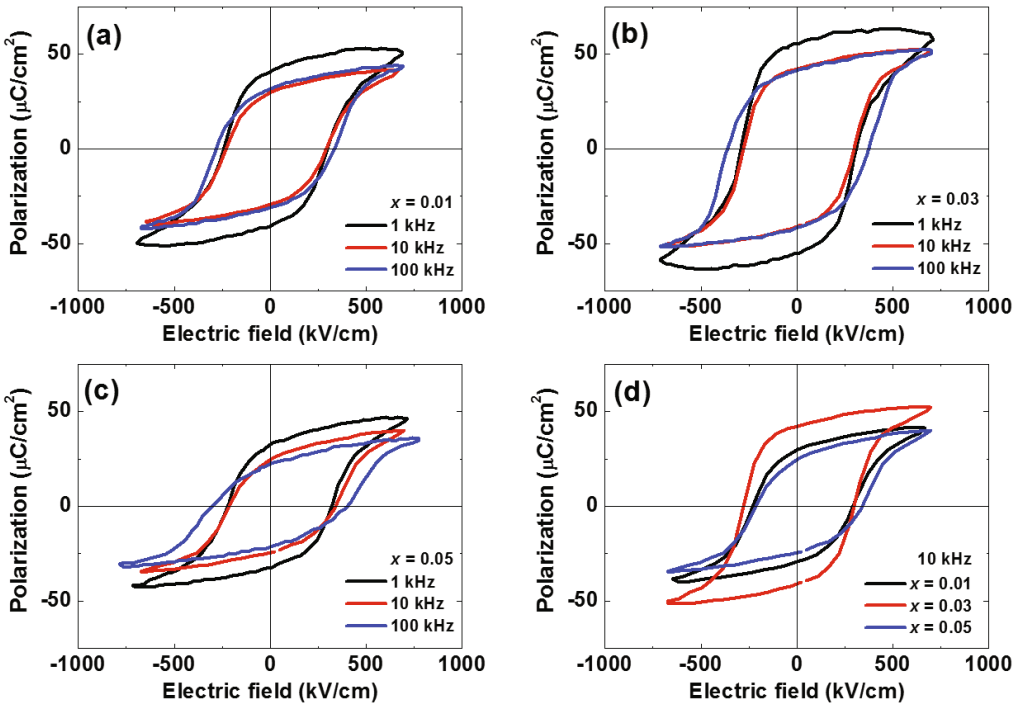

Fig. 5. (Color online) Ferroelectric hysteresis loops of (a) $x = 0.01$, (b) $x = 0.03$, and (c) $x = 0.05$ $Bi(Fe_{0.99-x}Zn_{0.01}Mn_x)O_3$ thin-film capacitors measured by using a triangular voltage pulse with 1, 10, and 100 kHz, and (d) $Bi(Fe_{0.99-x}Zn_{0.01}Mn_x)O_3$ ($x = 0.01$, 0.03, 0.05) thin-film capacitors measured at a 10 kHz triangular voltage pulse.

position method. The effects of Zn^{2+} and Mn^{4+} doping on the leakage current density and the ferroelectric properties of BFO thin films were investigated. A reduced leakage current density was observed in $Bi(Fe_{0.99-x}Zn_{0.01}Mn_x)O_3$ ($x = 0.01$, 0.03, 0.05) thin-film capacitors compared to BFO thin-film capacitor. Among them, the $Bi(Fe_{0.96}Zn_{0.01}Mn_{0.03})O_3$ thin film capacitor showed the lowest leakage current density and the largest remnant polarization because of the small Fe^{2+} concentration associated with oxygen vacancies and the large grain size. This result implies that controlling the contents of Zn^{2+} and Mn^{4+} in BFO thin films is important for reducing the leakage current and improving the ferroelectric properties.

ACKNOWLEDGMENTS

This research was financially supported by the National Institute for Nanomaterials Technology (NINT) in 2013.

REFERENCES

[1] J. Wang *et al.*, Science **299**, 1719 (2003).
[2] G. Catalan and J. F. Scott, Adv. Mater. **21**, 2463 (2009).
[3] G. W. Pabst, L. W. Martin, Y.-H. Chu and R. Ramesh, Appl. Phys. Lett. **90**, 072902 (2007).
[4] X. Qi, J. Dho, R. Tomov, M. G. Blamire and J. L. MacManus-Driscoll, Appl. Phys. Lett. **86**, 062903 (2005).
[5] J. M. Park, F. Gotoda, S. Nakashima, T. Kanashima and M. Okuyama, Cur. Appl. Phys. **11**, S270 (2011).
[6] M. H. Lee *et al.*, J. Korean Phys. Soc. **60**, 272 (2012).
[7] Y. Wang and C.-W. Nan, Appl. Phys. Lett. **89**, 052903 (2006).
[8] J. Wu, J. Wang, D. Xiao and J. Zhu, J. Appl. Phys. **109**, 124118 (2011).
[9] D. Do *et al.*, Ferroelectrics **454**, 57 (2013).
[10] G. D. Hu, S. H. Fan, C. H. Yang and W. B. Wu, Appl. Phys. Lett. **92**, 192905 (2008).
[11] D. Do, J. W. Kim, S. S. Kim, W.-J. Kim, M. H. Lee and T. K. Song, J. Korean Phys. Soc. **57**, 1875 (2010).
[12] R. D. Shannon, Acta Cryst. A **32**, 751 (1976).